Fabrication and RF test of large-area MgB_2 films on niobium substrates

Zhimao Ni[1], Xin Guo[1], Paul B. Welander[2], Can Yang[3], Matthew Franzi[2], Sami Tantawi[2], Qingrong Feng[3], Kexin Liu[1,*]

[1] School of Physics and State Key Laboratory of Nuclear Physics and Technology, Peking University, Beijing 100871, People's Republic of China

[2] SLAC National Accelerator Laboratory, Menlo Park, CA 94025, USA

[3] School of Physics and State Key Laboratory for Artificial Microstructure and Mesoscopic Physics, Applied Superconductivity Research Center, Peking University, Beijing 100871, People's Republic of China

* Corresponding author. E-mail address: kxliu@pku.edu.cn

Abstract

Magnesium diboride (MgB_2) is a promising candidate material for superconducting radio-frequency (SRF) cavities because of its higher transition temperature and critical field compared with niobium. To meet the demand of RF test devices, the fabrication of large-area MgB_2 films on metal substrates is needed. In this work, high quality MgB_2 films with 50-mm diameter were fabricated on niobium by using an improved HPCVD system at Peking University, and RF tests were carried out at SLAC National Accelerator Laboratory. The transition temperature is approximately 39.6 K and the RF surface resistance is about 120 μΩ at 4 K and 11.4 GHz. The fabrication processes, surface morphology, DC superconducting properties and RF tests of these large-area MgB_2 films are presented.

1. Introduction

Due to its exceptional superconducting properties, MgB_2 [1] is expected to have a

wide array of applications, including magnetic resonance imaging (MRI) magnets [2] and Josephson junctions and digital circuits [3]. Another important potential application is to fabricate superconducting radio frequency (SRF) cavities for particle accelerators [4-8]. An MgB_2-coated cavity would have two advantages compared with a bulk niobium (Nb) cavity. First, its high transition temperature (T_c) of 39 K enables accelerator operation well above 4 K, thereby substantially reducing the operation cost [9]. Second, the superheating critical field of MgB_2 is expected to be much higher than that of Nb, which could allow accelerating gradients well beyond the theoretical limit of Nb cavities [4, 10].

Extensive research has been performed regarding the deposition of MgB_2 films for superconducting resonant cavities [5, 11-14]. Early efforts were mainly focused on improving the quality of small-area (about 10×10 mm^2) MgB_2 films fabricated by different methods and on different substrates – e.g. sapphire [15, 16], Nb [17], Cu [18, 19], stainless steel (SS) [20] and Mo [11]. Recently, large-area MgB_2 films have been fabricated to meet the demand of RF test devices [21, 22], in which the MgB_2 coating is a part of the test cavity. Large-area MgB_2 films were deposited on various substrates up to 4 inches in diameter by reactive evaporation [23]. Later, 50-mm diameter MgB_2 films were successfully grown on sapphire substrates using a modified hybrid physical-chemical vapor deposition (HPCVD) method with a pocket heater [24] and scaled-up HPCVD method with a resistive heater [25].

We have fabricated high quality MgB_2 films with 50 mm diameter on Nb substrates using a HPCVD method at Peking University. The cryogenic RF tests have been carried out at SLAC National Accelerator Laboratory and the results are promising. In this paper, we present the fabrication process, superconducting properties, RF tests and results of the large-area MgB_2 films.

2. Fabrication of Large-area MgB_2 films

Large-area MgB_2 films were fabricated with a modified HPCVD system at the

Applied Superconductivity Research Center at Peking University. HPCVD, which takes advantage of both a high Mg vapor pressure and a clean environment, is an effective method to obtain high quality MgB_2 films with higher T_c and lower residual resistivity [6, 26]. In particular, it is considered a suitable way to fabricate MgB_2 films on the inner surfaces of cavities [27]. The modification of our HPCVD system includes enlarging the reactor chamber and fabricating a new susceptor with shield wall. A water-cooled, stainless steel cylindrical reactor chamber, 100 mm in diameter, encloses a 75-mm diameter molybdenum susceptor which is heated by a resistive tungsten coil. The substrate is placed in the center of the susceptor, surrounded with several pieces of Mg ingot. The initial experiments with the above structure showed poor results – the Mg vapor distribution above the substrate was found to be non-uniform, resulting in very poor crystallinity and connectivity of MgB_2 grains at the center area of the film. To address this problem, a wall about 9 mm in height was added surrounding the susceptor, improving the uniformity of Mg vapor above the substrate. Figure 1 shows the schematic of the improved HPCVD system.

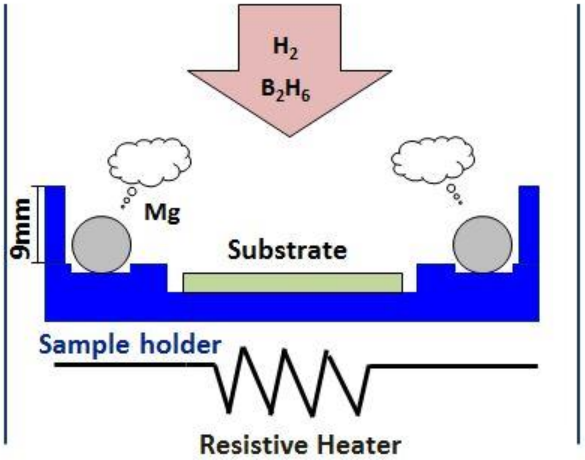

Figure 1. Schematic of the HPCVD system

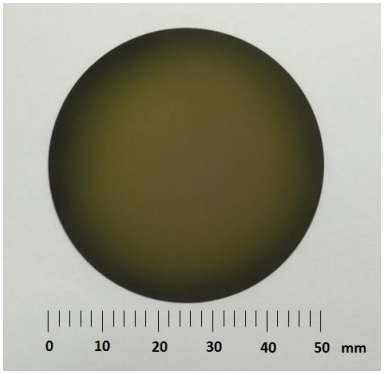

Figure 2. The picture of a large-area MgB_2 film

For our experiments, we used polycrystalline Nb substrates of 99.95% purity from Baoji Yunjie Metal Production Co., Ltd., China. Prior to film growth, the Nb substrates were mechanically polished to attain a surface roughness of 0.4 μm. The Mg ingot was also scraped to remove the surface oxidation layer. In the experiment, hydrogen was used as the background gas at a flow rate of 300 sccm and a pressure of 5.3 kPa to provide a reducing reaction environment. With the Mg ingot melted at about 680 °C, a mixed gas of 75% B_2H_6 and 25% H_2 (at a flow rate of 10 sccm) was introduced into the chamber. Film deposition occurs as boron decomposes from the B_2H_6 gas and reacts with the Mg vapor. After about 15 minutes the resulting MgB_2 film shows an average thickness of about 1.2 μm (see Figure 2).

Small pieces were cut from the 50-mm diameter MgB_2 films for performing x-ray diffraction (XRD) analysis, scanning electron microscopy (SEM), and DC electrical measurements. The XRD analysis was performed using a Rigaku X-ray diffractometer. An FEI NOVA Nano SEM 430 was used to characterize the MgB_2 surface morphology.

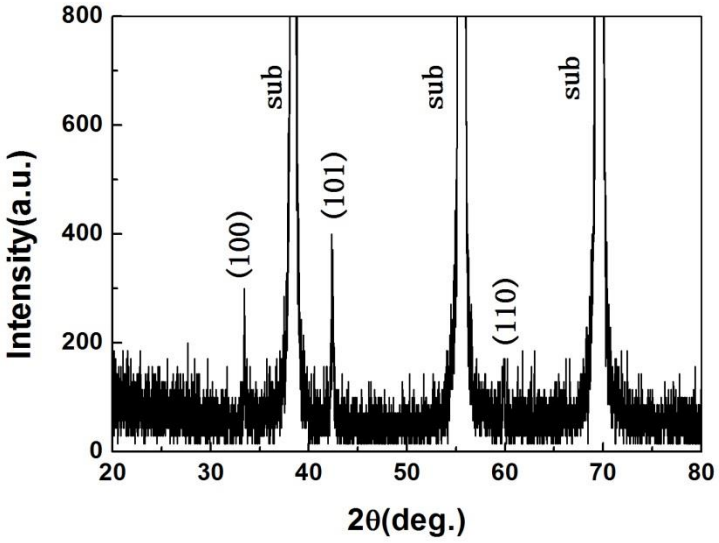

Figure 3. The X-ray diffraction pattern of the 50 mm-diameter MgB_2 film on Nb substrate.

Figure 3 shows a typical XRD pattern for our MgB_2 films on Nb substrates. The (101), (100) and (110) peaks indicate a polycrystalline film structure, which is different from epitaxial MgB_2 on sapphire or SiC substrates which display only (001) and (002) peaks [25, 28]. It is encouraging that there are no obvious impurity peaks (such as MgO) which have been observed previously in MgB_2 films on metal substrates [11, 17]. We speculate that the oxidation of magnesium was effectively suppressed by the relatively higher H_2 flow rate in our HPCVD process.

The surface morphology of a MgB_2 film measured by SEM is shown in Figure 4. The c-axes of part MgB_2 grains are parallel to the substrate surface, and others have small angles with the substrate surface. The size of MgB_2 grains in our film is around 1 μm in the ab-plane, larger than that of MgB_2 grains fabricated on sapphire which are approximately 150 nm in the ab-plane [25]. According to BCS theory, surface resistance is proportional to the square root of residual resistivity [8, 29]. The MgB_2 film with large grains has relatively low residual resistivity which is influenced by the scattering at the grain boundaries [23]. Thus our MgB_2 films may have low surface resistance, which is benefit to the application of SRF cavities.

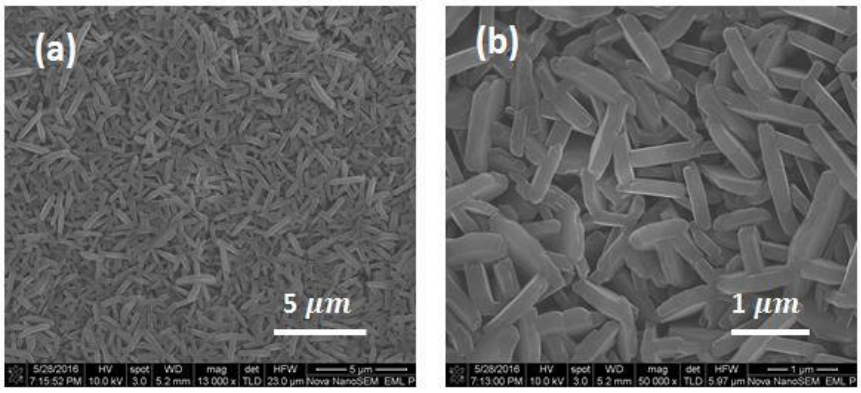

Figure 4. SEM images of the 50-mm diameter MgB_2 film on Nb substrate. (a) Characteristics surface morphology of the film with 13 000 magnification. (b) The image of the surface morphology with higher magnification of 50 000.

3. DC superconducting properties

Resistance versus temperature (R-T) measurements were performed using the standard four-probe method, and magnetization hysteresis loops (M–H) were recorded with a Quantum Design MPMS-7. The critical current density in a magnetic field $J_c(H)$ was calculated using the Bean model.

To check the uniformity of a 50-mm diameter MgB_2 film, five rectangular pieces (2×10 mm^2) were cut from a 2-mm belt region along the diameter. Figure 5 shows the variations of resistance versus temperature for these five small samples. Here, the resistance includes the contribution from the MgB_2 film and the conductive substrate. Both the T_c and the transition widths, ΔT, of each sample are listed in Table 1. T_c is the temperature when resistance is 90% of the normal state resistance at the transition point, and ΔT is the temperature difference between 90% and 10% of that resistance. T_c ranges from 38.4 K to 40.6 K, and ΔT ranges from 0.3 K to 1.3 K, which shows good uniformity of the film's superconducting properties and connectivity across the large film area. The T_c of our large-area MgB_2 film is comparable to those of small-area films on metal substrates such as Nb [17] and large-area films on sapphire [25].

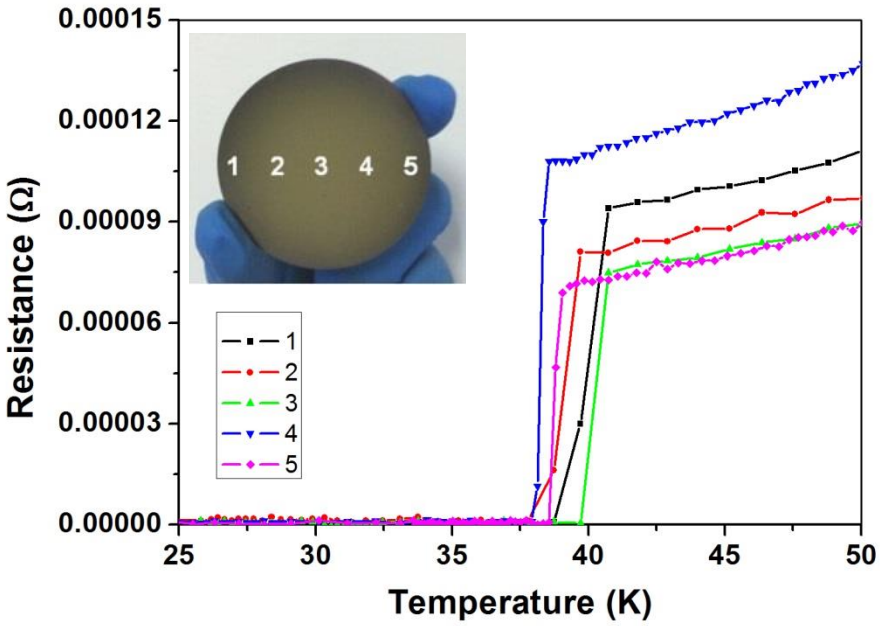

Figure 5. Resistance versus temperature for the five samples cut from the 50 mm-diameter MgB_2 film on Nb substrate. The inset shows a picture of the 50 mm-diameter MgB_2 film on Nb substrate.

Table 1. The T_c and ΔT values for the samples at different positions of the 50 mm-diameter MgB_2 film (The numbers corresponded to the positions of the film were marked in picture of the film shown in the inset of figure 5)

Sample number	**1**	**2**	**3**	**4**	**5**
T_c/K	40.6	39.6	40.6	38.4	39.0
ΔT/K	1.3	0.9	0.8	0.3	0.4

Figure 6 exhibits the field dependence of critical current density (J_c) obtained from magnetization hysteresis (M-H) loops at temperatures of 10 K and 20 K. J_c is calculated by using the Bean model $J_c = 20\Delta M/[Va(1 - a/3b)]$, where ΔM is the difference between the upper and lower magnetization amplitude at the same magnetic field; V is the volume of the MgB_2 film; a and b are the sample dimensions with a < b. The J_c values at self-field are about 4.1×10^5 A/cm^2 and 2.7×10^5 A/cm^2 at 10 K and 20 K, respectively. J_c values of our MgB_2 film on Nb are lower compared with the epitaxial films on

sapphire [25]. The lower J_c value may be due to the larger grain size of our films, resulting in fewer grain-boundary pinning centers.

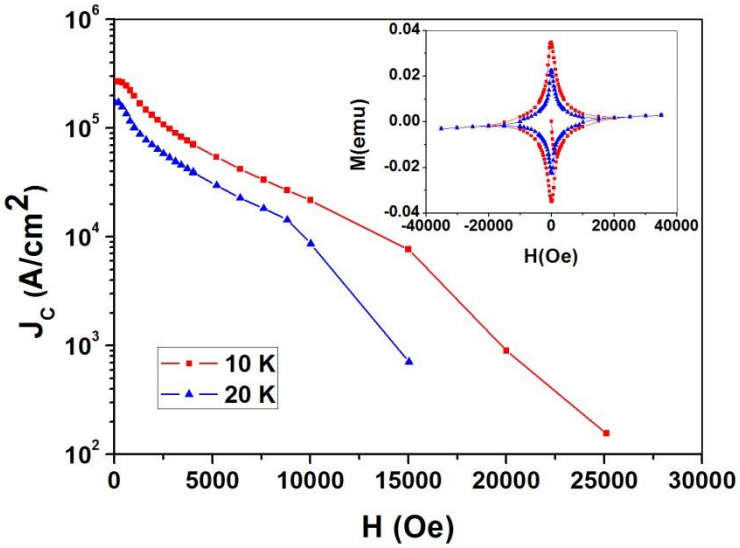

Figure 6. J_c versus field at 10 K and 20 K obtained from M-H loops by using the Bean model. The inset shows the M-H loops for the MgB_2 film

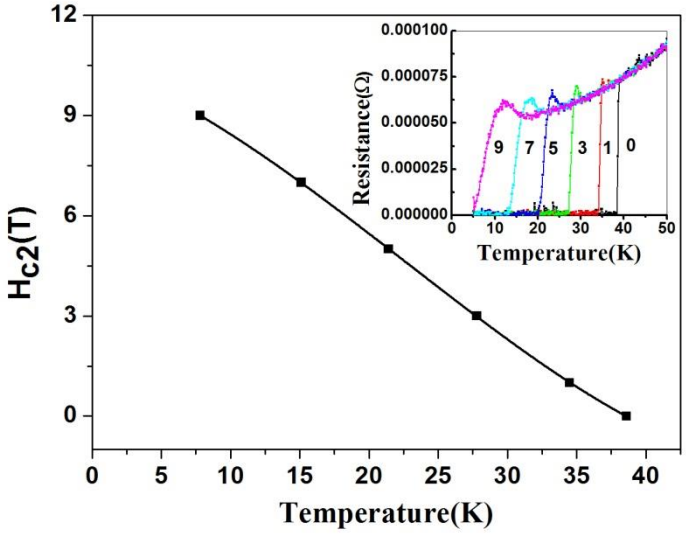

Figure 7. Upper critical field H_{c2} versus temperature for the MgB_2 film on Nb substrate. The inset shows the temperature-dependent resistance measurements under magnetic field up to 9 T.

The upper critical field, H_{c2}, versus temperature is plotted in Figure 7, which was

obtained from the temperature-dependent resistance measurements. In our experiments, T_c was measured with different applied magnetic fields from 0 to 9 T. Thus each setting magnetic field is H_{c2} at the temperature of corresponding T_c. Here, the T_c is also determined from the R-T measurements with the 90% criterion. Extrapolating to 0 K, we find an $H_{c2}(0)$ of 10.6 T, lower than what is typically found for MgB_2 films on metal substrates – e.g. 15.3 T on Cu [18], 15.2 T on stainless steel [20] and 13.5 T on Mo [12]. It is stated that $H_{c2}(0)$ increases when the MgB_2 films are dirty [6, 25], suggesting our film is likely cleaner than previous MgB_2 films on different metal substrates, which correlates well with our XRD analysis in Section 2. However, considering that this kind of extrapolation is potentially highly erroneous for a multi-band and multi-gap superconductor such as MgB_2 [30], and H_{c2} of MgB_2 film is also related to orientations, boundaries and lattice parameters of grains except impurities [6], above comparison is fairly rough. $H_{c2}(0)$ of our film is higher than 7 T which is the extrapolating value of the clean c-axis epitaxial MgB_2 film on sapphire [6, 25]. One reason for this higher $H_{c2}(0)$ is the different orientation of grains. Our MgB_2 films are polycrystalline with most grains having the c-axis parallel with substrate surface, which means the magnetic field was applied in perpendicular to the c-axis for most of the grains. Another possible contribution is that some defects or impurities are still present in our MgB_2 film on Nb.

4. RF tests and results

RF tests for the 50-mm diameter MgB_2 films fabricated on Nb substrates were carried out at SLAC National Accelerator Laboratory. At SLAC, a second-generation X-band cavity cryostat has been commissioned for the rapid analysis of superconducting materials [22]. Two hemispherical cavities (one Cu, one Nb-coated Cu) are utilized in the system, with 2-inch samples mounted on the flat surface of the cavities. The cavities operate at 11.4 GHz with a TE_{032}-like mode where the magnetic field is strongest on the sample surface. By measuring the unloaded quality factor, Q_0, at different temperatures,

T_c of the sample can be obtained with the Cu cavity (copper has no transition temperature), while the surface resistance, R_s, can be resolved with the Nb cavity – the Nb R_s is only about 1% of the Cu value at 4 K and 11.4 GHz. Figure 8 shows the variation of the Cu cavity Q_0 with our MgB_2 film versus temperature. T_c of the MgB_2 film, which determined by measuring where Q flattens out at high temperature, is about 39 K and consistent with the average value from our DC R-T analysis. It is clear from Figure 8 that the cavity Q_0 has no obvious variation from 4 K to about 25 K. This means that the MgB_2 film has low R_s at a wide range of temperatures above 4 K.

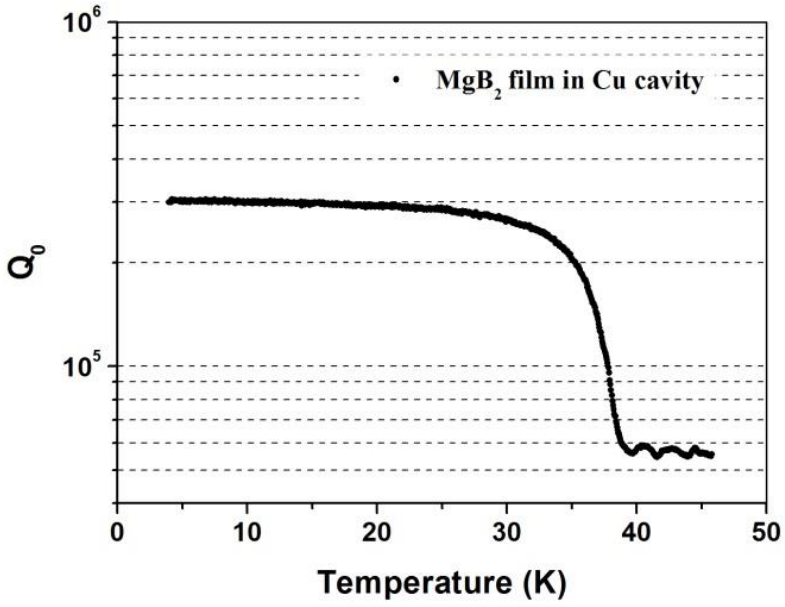

Figure 8 Quality factors versus temperature at 11.4 GHz for a 50 mm-diameter MgB_2 film measured in a Cu cavity

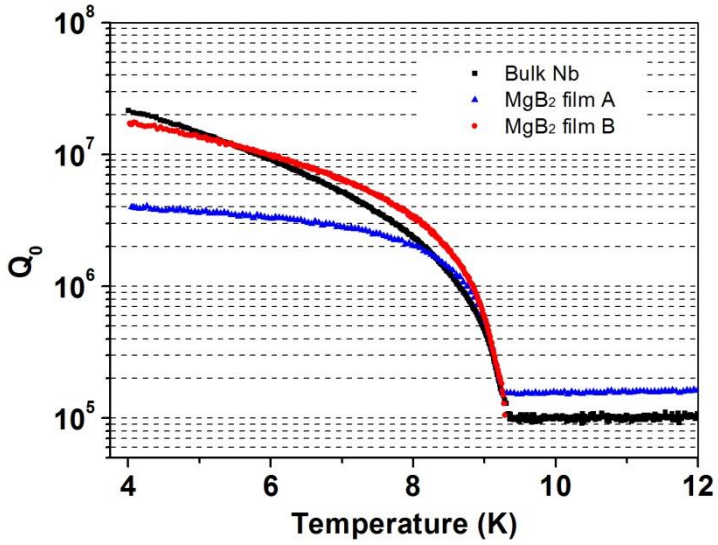

Figure 9. Quality factors versus temperature at 11.4 GHz for two 50-mm diameter MgB_2 films (blue triangle and red circle) and a bulk Nb wafer as reference (black squares) measured in the Nb-coated cavity.

Figure 9 shows Q_0 versus temperature for the Nb-coated cavity with two 50-mm diameter MgB_2 films, along with a bulk Nb reference sample. Films A and B are MgB_2 films deposited on Nb substrates with surface roughnesses of 1 μm and 0.4 μm, respectively. R_s of the total cavity, which reflects the RF dissipation, is a linear combination of the cavity body surface resistance, R_{cavity}, and the sample surface resistance, R_{sample}. R_{sample} can be derived from the equation $Q_0 = G_{total}/(0.67R_{cavity} + 0.33R_{sample})$ [22], where G_{total} is the geometrical factor of the total cavity, and the participation ratios are determined by relating the geometrical factors for the cavity body and sample to G_{total}. R_{cavity} for the Nb-coated Cu cavity is estimated to be 65 μΩ, which gives R_s values for films A and B of about 930 μΩ and 120 μΩ at 4 K, respectively.

It seems that roughness of the substrate surface strongly affects the MgB_2 R_s. Films fabricated on a rough surface are more easily populated with V-shape voids between the MgB_2 grains, which may cause R_s to increase. On the other hand, MgB_2 films fabricated on smooth substrate surfaces can have a lower R_s because of the high grain density. Since

the surface resistance of MgB_2 films may also be affected by film thickness [31], we have investigated the uniformity of thickness and homogeneity of DC superconducting properties of a MgB_2 film C which has the same substrate surface roughness of the film A. Figure 10 shows a typical cross section view of the film C observed by SEM and R-T curves of five samples cut from a belt region along the diameter of the film C. The distance between "peaks" is larger than the height of the "peaks" and there is no big difference of MgB_2 film thickness at "peak" and "valley" of the substrate surface. In addition, almost the same T_c for five samples indicates a good homogeneity in superconducting properties of the film C. Therefore, the large surface resistance of the film A is mainly caused by the large surface roughness of the substrate.

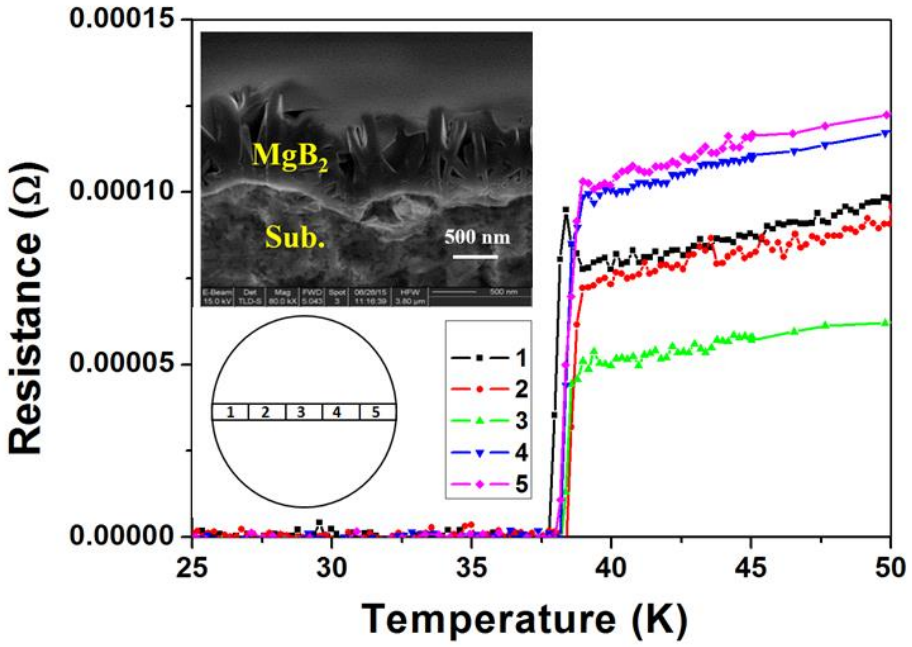

Figure 10. R-T measurements of the film C. The upper insert is a cross-sectional SEM image of the film C

The R_s measurement result of 120 μΩ at 4K and 11.4 GHz is promising. The lowest R_s of MgB_2 films fabricated on sapphire are 20 μΩ at 4.2 K and 10 GHz reported by

Moeckly et al. [32] and 9 μΩ at 2.2K and 7.4 GHz reported by Xiao et al. [31]. However, films on metal substrates are polycrystalline rather than epitaxial for MgB_2 films on single crystalline substrates, which may yield a larger R_s. The lowest R_s of MgB_2 films fabricated on metal substrates by the method of reactive evaporation is about 1 μΩ at 5 K and 2.2 GHz reported by Oates et al. [7]. Our R_s result for MgB_2 film B is comparable with above lowest R_s using the well-known f^2 scaling rule of the surface resistance. On the other hand, comparing R_s of film B with the bulk Nb sample, R_s of the MgB_2 film (~ 120 μΩ) is roughly twice that of bulk Nb (~ 65 μΩ) at 4 K. Furthermore, there is a cross-over point at about 5.5 K in figure 9, above which the MgB_2 film exhibits lower R_s compared with bulk Nb. This means that our MgB_2 film on Nb substrate fabricated by HPCVD has an essential quality for the application to accelerator cavities.

5. Conclusion

To study the RF properties of MgB_2 films for their application in SRF cavities, we have fabricated large-area MgB_2 films on 50-mm diameter Nb substrates by HPCVD, which has an essential quality for the application to accelerator cavities. The MgB_2 films have a polycrystalline structure with (101), (100) and (110) orientation, and large grains of around 1 μm along the ab-plane. T_c values measured at different positions on the film range from 38.4 K to 40.6 K, showing good film uniformity. The H_{c2} (0) of 10.6 T is lower than those of previous MgB_2 films on metal substrates. In RF tests, the film exhibits a low R_s of about 120 μΩ at 4 K and 11.4 GHz, close to that of bulk Nb. By further improving the cleanliness and density, MgB_2 films with lower R_s are expected.

Acknowledgments

This work was supported by the National Natural Science Foundation of China under Grant nos. 11575012 and 51177160, the National Basic Research Program of China

under Grant (973 program) nos. 2011CB808303 and 2011CBA00104, and the Zhejiang Provincial Natural Science Foundation under Grant no. LQ13E070002. Work at SLAC National Accelerator Laboratory was supported by the U.S. Department of Energy, contract no. DE-AC02-76SF00515.

Reference

[1] Nagamatsu J, Nakagawa N, Muranaka T, Zenitani Y and Akimitsu J 2001 *Nature* **410** 63-4
[2] Iwasa Y, et al., 2006 *IEEE Trans. Appl. Supercond.* **16** 1457-64
[3] Ueda K, et al., 2005 *Appl. Phys. Lett.* **86** 172502.
[4] Collings E W, Sumption M D, Tajima T, 2004 *Supercond. Sci. Technol.* **17** S595-601.
[5] Tajima T, Canabal A, Zhao Y, et al., 2007 *IEEE Trans. Appl. Supercond.* **17** 1330-3
[6] Xi X X, 2009 *Supercond. Sci. Technol.* **22** 043001
[7] Oates D E, Agassi Y D, Moeckly B. H, 2010 *Supercond. Sci. Technol.* **23** 034011
[8] Valente-Feliciano A M, 2016 *Supercond. Sci. Technol.* **29** 113002
[9] Nassiri A, et al., 2013 *Proc. 16th Int. Conf. on RF Superconductivity (Paris)* TUP086
[10] Catelani G, Sethna J, 2008 *Physical Review B,* **78** 224509
[11] Mitsunobu S, Inagaki H, et al., 2009 *Proc. 16th Int. Conf. on RF Superconductivity (Berlin)* TUPPO077.
[12] He F, Xie D T, Feng Q R and Liu K X, 2012 *Supercond. Sci. Technol.* **25** 65003
[13] Zhuang C, Tan T, Krick A, et al., 2013 *J. Supercond. Nov. Magn.* **26** 1563-8.
[14] Guo X, Ni Z M, Chen L Z, et al., 2016 *Physica C* **524** 13-7
[15] Tian W and Pan X Q, 2002 *Appl. Phys. Lett.* **81** 685-7.
[16] Kang S G, Park S C,Chung J K, et al., 2009 *Physica C* **469** 1571-3.
[17] Zhuang C G, Yao D, Li F, et al., 2007 *Supercond. Sci. Technol.* **20** 287–91.
[18] Li F, Guo T, Zhang K, et al. 2006 *Supercond. Sci. Technol.* **19** 1196-9
[19] Lee T G, et al., 2009 *Supercond. Sci. Technol.* **22** 045006.
[20] Li F, Guo T, Zhang K, Chen C and Feng Q R 2007 *Physica C* **452** 6-10
[21] Xiao B P, Reece C E, Phillips H L, et al. 2011 *Rev. Sci. Instrum.* **82** 056104
[22] Welander P B, Franzi M, Tantawi S, 2015 *Proc. 17th Int. Conf. on RF Superconductivity (Whistler)* TUPB065
[23] Moeckly B H and Ruby W S, 2006 *Supercond. Sci. Technol.* **19** L21–4
[24] Wang S F, Chen K, et al. 2008 *Supercond. Sci. Technol.* **21** 085019
[25] Tan T, Zhuang C G, Krick A, et al. 2013 *IEEE Trans. Appl. Supercond.* **23** 7500304
[26] Zeng X, Pogrebnyakov A V, Kotcharov A, et al. 2002 *Nature Mater.* **1** 35-8
[27] Wolak M A, Tan T, Krick A, et al. 2014 *Phys. Rev. ST Accel. Beams* **17** 012001
[28] Li F, Guo T, et al., 2006 *Supercond. Sci. Technol.* **19** 1073–5
[29] Palmieri V, 2001 *Proc. 10th Int. Conf. on RF Superconductivity* (Tsukuba) 162-9
[30] Gurevich A, 2003 *Phys. Rev. B* **67** 184515
[31] Xiao B P, Zhao X, et al., 2012 *Supercond. Sci. Technol.* **25** 095006
[32] Moeckly B H, Kihlstrom K E, et al. 2005 *IEEE Trans. Appl. Supercond.* **15** 2